Size control and registration of nano-structured thin films by cross-linkable units

Eunhye Kim,[a] Changhak Shin,[a] Hyungju Ahn,[a] Du Yeol Ryu,*[a] Joona Bang,*[b] Craig J. Hawker[c] and Thomas P. Russell[d]

Received 19th November 2007, Accepted 21st December 2007
First published as an Advance Article on the web 9th January 2008
DOI: 10.1039/b717903k

Thermoset thin films *via* directed self-assembly, where benzocyclobutene (BCB) groups are incorporated selectively into the one block, have been prepared from cross-linkable block copolymers in a simple process, which allows size controllability and the registration of oriented microdomains in multi-layer applications.

Nanoscopic patterns prepared from the self-assembly of block copolymers (BCPs) have recently drawn considerable attention as a simple method for generating scaffolds and templates for nano-structured materials.[1–12] Depending upon the volume fraction of each block, the segmental interaction between two components, and the degree of polymerization (N), BCPs exhibit well-organized arrays of lamellar, cylindrical, gyroid, and spherical microdomains that are tens of nanometres in size.[13] By controlling interfacial interactions a simple route is opened to nano-structured arrays in the fabrication of multi-level thin film devices, since the balanced interfacial interaction allows the microdomains of the BCP to orient normal to the surface.[1,14–16] The use of oriented cylindrical microdomains of BCPs for lithography augments traditional photolithography for applications, including nano-lithographic templates,[2,10] etching masks,[3,4,12] nanowire fabrication,[5] nanoparticle deposition,[6] nanoporous membranes,[7] optical wave guides[8] and nano-textured surfaces.[9] For such applications, control over the microdomain size is of crucial importance for many of the desired practical uses.

To accomplish this control, the standard strategy was to control the average molecular weight of the cylinder-forming BCP such as polystyrene-*block*-polymethyl methacrylate (PS-*b*-PMMA) with the target microdomain size being dictated by the molecular weight of individual chains. However, at very high molecular weights (~150 000 g mol^{-1}), the limited mobility of the polymer chains leads to extremely slow ordering and a lack of lateral ordering with increased lattice spacing.[17] To overcome this limitation in obtaining a larger nano-structure matrix contraction by ozone exposure was explored, but only small changes in feature size (~3 nm) were observed.[18,19] In addition, this technique requires two additional process steps, ozone exposure to cross-link the PS matrix at room temperature and a second annealing step to relax the matrix above the glass transition temperatures (T_g), allowing only minimal ability to control pore size and separation.

Recent studies on accelerated strategies for surface neutralization have shown that functionalized copolymers offer a number of advantages. For example, the minimum effective thickness for thermally cross-linkable thin films of benzocyclobutene (BCB)-functionalized random copolymer with styrene and methyl methacrylate, P(S-*r*-BCB-*r*-MMA) is approximately 5.5 nm. This is the minimum thickness that prevents penetration of the BCP to the underlying substrate and above this thickness, the cross-linked BCB thin film can be effectively used to manipulate interfacial interactions in a straightforward manner, regardless of the nature of the substrate.[14,16] An additional advantage is that the BCB group can be used for cross-linkable BCPs, providing a means for obtaining structurally robust, thermoset nanostructures.[20]

In this study, a simple route to control the microdomain size in PS-*b*-PMMA by varying the amount of cross-linkable BCB unit is presented. PS-*b*-PMMA, with reactive BCB functionality in the PS block, denoted (PS-*r*-BCB)-*b*-PMMA (Scheme 1(a)), was synthesized

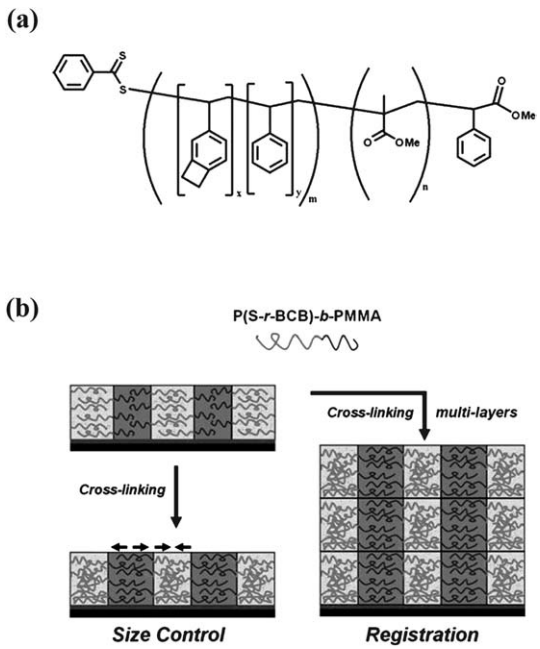

Scheme 1 (a) Molecular structure of (PS-*r*-BCB)-*b*-PMMA copolymers and (b) schematic for the cross-linking process and multi-layer registration of the BCP thin films. The benzocyclobutene (BCB) functionality is randomly incorporated into the PS block with the different BCB amounts (3.3, 6.6 and 9.7 mol%).

[a]*Department of Chemical Engineering, Yonsei University, Seoul, Korea. E-mail: dyryu@yonsei.ac.kr; Fax: +822 312 6401; Tel: +822 2123 5756*
[b]*Department of Chemical & Biological Engineering, Korea University, Seoul, Korea. E-mail: joona@korea.ac.kr*
[c]*Materials Research Laboratory, University of California, Santa Barbara, CA 93016, USA*
[d]*Department of Polymer Science & Engineering, University of Massachusetts, Amherst, MA 01003, USA*

by reversible addition fragmentation chain transfer (RAFT) polymerization.[21,22] The (PS-*r*-BCB)-*b*-PMMA copolymers were designed to yield cylindrical microdomains, with a total PS volume fraction of ~0.73, containing varying amounts of BCB (3.3, 6.6 and 9.7 mol% relative to S). The number-average molecular weights (M_n) of PS-*b*-PMMA were 81 300, 86 600, and 82 800 with polydispersity indices (PDI) of 1.08, 1.07 and 1.10, respectively. For comparison, PS-*b*-PMMA with no BCB (or 0 mol% BCB) was synthesized anionically with a PS volume fraction of 0.72 and a $M_n = 84\,000$, and a PDI of 1.06. Upon annealing at elevated temperatures, the BCB group undergoes a facile intra- and/or inter-molecular cross-linking reaction by ring opening, leading to thermoset polymer thin films.[23,24] (PS-*r*-BCB)-*b*-PMMA, hereafter referred to as PS-*b*-PMMA with BCB, maintains a stable structure due to the insoluble and intractable characteristics of thermoset materials. The elevated temperature for cross-linking the BCB group is also advantageous since no reaction is observed at lower temperature, allowing the BCPs to be thermally annealed and ordered into self-assembled nanostructures. All the BCP thin films in this study were prepared on a substrate where interfacial interactions of the PS and PMMA blocks with the substrate were balanced by anchoring a random copolymer brush to the substrate, having a 58 : 42 (mol%) composition of S : MMA on standard Si wafer. The thicknesses of the PS-*b*-PMMA film was ~30 ± 2 nm, as measured by ellipsometry (SE MG-1000, Nano-view Co.) at a 70° incident angle.[1,25]

In optimizing the processes, the BCP films were initially annealed at 150 °C for 3 days in order to avoid cross-linking reactions. However, imperfectly ordered microdomains were observed which can be attributed to the lack of chain mobility in the BCPs. Increasing the annealing temperature to 160 °C for one day produced ordered nanostructures for all the BCP thin films with the microdomains oriented normal to the surface, as shown in Fig. 1.

Fig. 1(a)–(d) shows TEM images of PS-*b*-PMMA thin films with different amounts of BCB, from 0 to 9.7 mol%, annealed at 160 °C for one day under vacuum. Scanning and transmission electron microscopy (STEM; Hitachi S-4800) was operated at 3 kV and 30 eV, respectively; the block copolymer thin films were detached off using a sacrificial oxide layer of 200 nm and stained with RuO_4 to enhance the electron density contrast of the thin films. With increasing amounts of BCB, it is seen that the diameter of the PMMA microdomains increases by 32%, from 22 nm (0 mol% BCB) to 29 nm (9.7 mol% BCB), which suggests that partial cross-linking occurred at 160 °C and increased with increasing amounts of BCB. An entirely cross-linked PS matrix could be prepared when all thin films were annealed at 160 °C and subsequently cross-linked at 250 °C for 15 min under N_2 flow, as shown in Fig. 1(e)–(h) and descried in Scheme 1(b). The density of the cross-links, of course, increases with increasing amounts of BCB. As can be seen, the microdomain size increased during the volume contraction of the PS matrix by BCB cross-linking, with the PMMA microdomains remaining oriented normal to the film surface even in the thin films with 9.7 mol% BCB. In the case of thin films with larger amounts of BCB (9.7 mol%), however, minor defects, like connected microdomains, were observed, indicating that the excess cross-linkable BCB group in the PS matrix hindered the ordering of the PMMA microdomains above T_g, as shown in Fig. 1(d) and (h). The TEM images in Fig. 1 were found to be consistent with the phase images from scanning probe microscopy (SPM).

Domain sizes in the PS-*b*-PMMA thin films were measured by tapping-mode SPM (Dimension 3100, Digital Instrument Co.), rather than TEM, to avoid artifacts that may occur in the interpretation of the TEM images. Domain sizes, measured after thermal annealing at 160 °C and after subsequent cross-linking at 250 °C are plotted in Fig. 2 as a function of mol% BCB in the PS matrix. An increase in the domain size after thermal annealing at 160 °C is seen with increasing amounts of BCB, indicating that a partial cross-linking occurred due to the highly reactive BCB groups. Such behavior was enhanced for PS-*b*-PMMA thin films with larger amounts of BCB (9.7 mol%) with only minor perturbation of the perpendicular orientation.

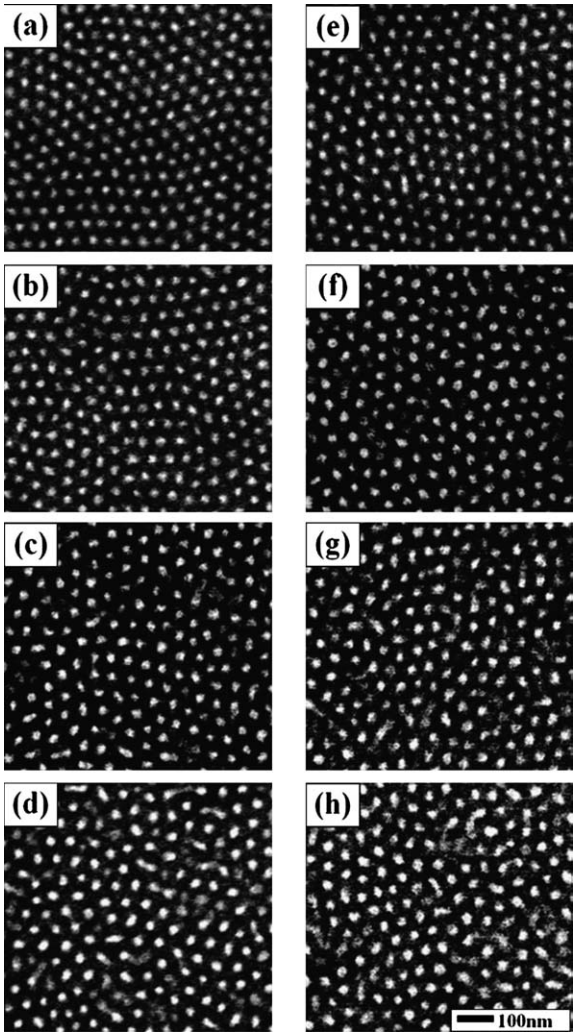

Fig. 1 TEM images of PS-*b*-PMMA thin films with varying BCB amounts (0, 3.3, 6.6 and 9.7 mol%). The left and right images were taken from thin films annealed at 160 °C for one day and subsequently cross-linked at 250 °C for 15 min. The microdomains of the PS-*b*-PMMA were oriented normal to the surface due to the balanced interfacial interaction on the surface by the random copolymer brush.

This can be attributed to the different density of cross-links resulting from the different amounts of BCB. However, sufficient chain mobility for BCP ordering was attained at this temperature as shown in Fig. 1(a)–(d). It should be noted that the PS-*b*-PMMA thin films annealed at 160 °C showed an orientation of cylindrical microdomains normal to the surface, while partial cross-linking also occurs at 160 °C although minor.

The thin films were further heated to 250 °C for 15 min, as described in Scheme 1(b), to fully cross-link the BCB groups, resulting

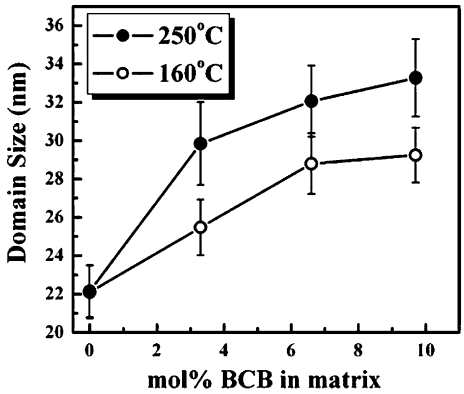

Fig. 2 Domains size of PS-*b*-PMMA thin films with varying BCB amounts (0, 3.3, 6.6 and 9.7 mol%), annealed at 160 °C for one day and then further cross-linked at 250 °C for 15 min to prepare the entirely cross-linked thin films.

in robust thermoset BCP thin films. This process leads to a ~14.1% increase in the domain size of the PMMA due to a contraction of the PS matrix by cross-linking. In contrast, the domain size of non-functionalized PS-*b*-PMMA thin films with no BCB remained unchanged. Consequently, the thermal cross-linking provides two routes to control the size of the copolymer microdomains, namely: (1) by controlling the amount of BCB in the PS block, or (2) by limiting the extent of cross-linking.

Detailed structural characterization of the PS-*b*-PMMA thin films was obtained using grazing-incidence small-angle X-ray scattering (GISAXS) to probe the internal structure.[26,27] Experiments were carried out at the 4C1 and 4C2 beam-lines at the Pohang Accelerator Laboratory (PAL), Korea. 2D GISAXS patterns were recorded using a CCD detector positioned at the end of a vacuum guide tube when the X-rays pass through the BCP thin films under vacuum (5×10^{-4} Torr), where the operating conditions were set to a wavelength of 1.38 Å and a sample-to-detector distance of 2.19 m. Fig. 3 (a)–(h) shows GISAXS profiles of PS-*b*-PMMA thin films annealed at 160 °C (lhs) for one day and, then, further cross-linked at 250 °C (rhs) for 15 min with the different amounts of BCB; 0 mol% (a, e), 3.3 mol% (b, f), 6.6 mol% (c, g), and 9.7 mol% (d, h). The intensity profiles of the GISAXS patterns scanned along q_y are given at the bottom of Fig. 3 to compare internal ordering in the thin films. By exposing the films to UV, followed by rinsing with acetic acid, the PMMA was removed, leaving a cross-linked nanoporous film. The removal of the PMMA also increases the X-ray contrast significantly, by increasing the intensity of the scattering. In the scattering geometry, q_y is the momentum transfer normal to the incident plane, where *d*-spacing is related to q_y by $d = 2\pi/q_y$. The term q_z is the momentum transfer normal to the sample surface, defined as $q_z = (4\pi/\lambda)\sin\theta$, where λ is the wavelength of the X-rays and 2θ is the scattering angle. Incident angles were set at 0.2°, which is above the critical angle (0.135°) of PS-*b*-PMMA films. At this incident angle, the X-rays penetrate the entire film probing the internal structures of the film.

PS-*b*-PMMA films, annealed at 160 °C and subsequently cross-linked at 250 °C, (Fig. 3(a) and (e), respectively), showed a sharp first-order peak at $q_y = 0.181$ nm^{-1} with higher-order peaks at constant $q_z = 0.318$ nm^{-1} corresponding to hexagonally packed cylindrical microdomains, with an average *d*-spacing distance of 34 nm ($d = 2\pi/q_y$) oriented normal to the surface at scattering vector ratios of $1 : \sqrt{3} : \sqrt{4} : \sqrt{7} : \sqrt{9}$ relative to the first-order peak. The sharpness

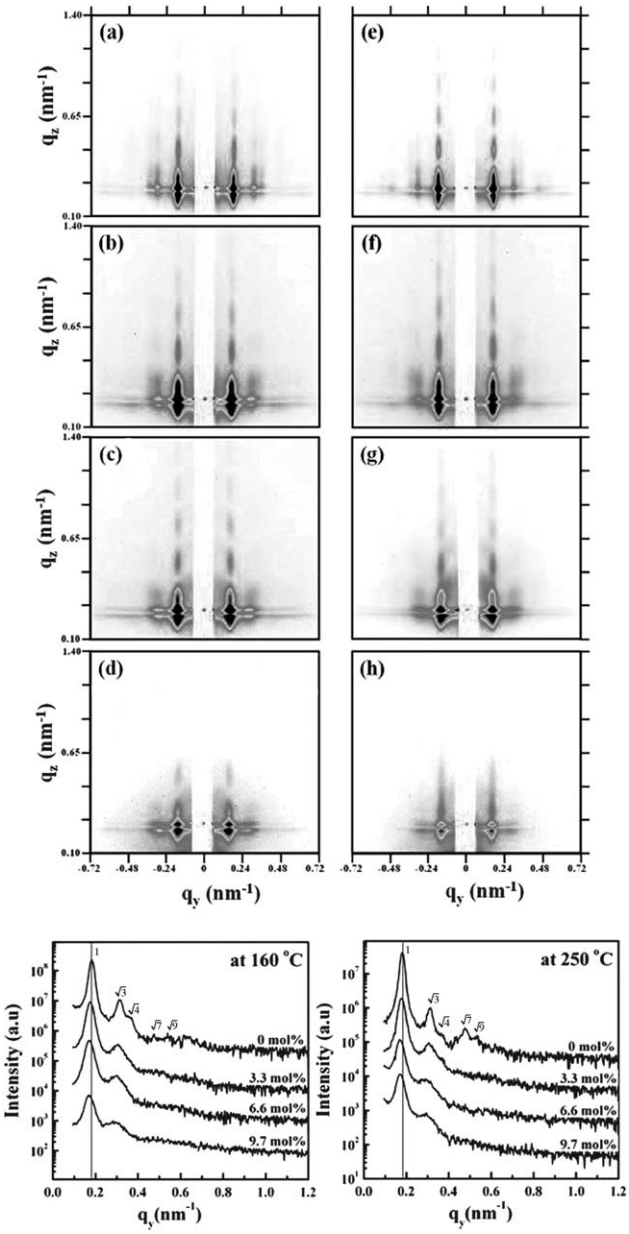

Fig. 3 Two-dimensional GISAX patterns measured at a 0.2° incident angle of PS-*b*-PMMA thin films after thermal annealing at 160 °C (a)–(d) and then further cross-linked at 250 °C (e)–(h) with different BCB amounts; 0 mol% (a, e), 3.3 mol% (b, f), 6.6 mol% (c, g), and 9.7 mol% (d, h). Intensity profiles (bottom figures) were scanned at $q_z = 0.318$ nm^{-1} as a function of q_y. To increase the scattering contrast PMMA microdomains were removed from all thin film samples by UV exposure and subsequent rinsing with acetic acid.

of the first- and higher-order peaks for the PS-*b*-PMMA thin film with 3.3 mol% BCB and 6.6 mol% BCB annealed at 160 °C (b, c) and cross-linked at 250 °C (f, g) indicates that the cylindrical microdomains are oriented normal to the film surface, suggesting that the cross-linking of the PS block did not interfere with the ordering and orientation of the copolymer. However, as shown in Fig. 1(d) and (h), the scattering peaks of the film with 9.7mol% BCB in Fig. 3 (d) and (h) showed a lower intensity for the first-order peak and broader higher-order peaks, indicating that the cross-linking reaction

is beginning to interfere with the ordering and orientation of the copolymer microdomains due to the predominant reaction of the excess cross-linkable BCB groups in the PS matrix before ordering.

The GISAXS patterns above the critical angle agreed with the measurements below the critical angle with the ordering and orientation of the microdomains normal to the film surface being seen for all concentrations of BCB, however, at higher BCB levels of incorporation, both order and orientation began to decrease. It should also be noted that the *d*-spacing increased from 34.5 nm to 37 nm with increasing amounts of BCB, irrespective of the annealing temperature, which is proportional to the density of cross-links or the amount of BCB in the BCP. Accordingly, it is observed that the film thickness decreased up to 1.8% (or 5.3 vol%) with increasing BCB amount in comparison to that of PS-*b*-PMMA with no BCB, which is attributed to volume contraction due to effective cross-linking.

A remarkable advantage of the cross-linkable PS-*b*-PMMA thin films is their insolubility when the samples are cross-linked at higher temperature (250 °C), which allows their subsequent use in further processes, such as the fabrication of 3-dimensional multi-layered arrays, that exploit directed self-assembly for adjacent layers. Once the cross-linked thin films are prepared, the resulting thin films of PS-*b*-PMMA are insoluble and hence the next layer can be fabricated on underlying cross-linked thin films *via* a layer-by-layer fashion as described in Scheme 1(b). Fig. 4 shows the cross-sectional schematics and their SEM images taken at a tilt angle of 55° to probe a cross-section of the multi-layered thin films of PS-*b*-PMMA with 3 mol% BCB. Here, the PMMA microdomains were removed by UV exposure and subsequent rinsing with acetic acid after multi-layer fabrication. From Fig. 4(a), it can be clearly seen that the cylindrical microdomains persisted throughout the entire thickness at 2 layers (~54 nm), suggesting that the microdomains of two consecutive layers were in register. This registration of the microdomain orientation persisted for at least 3 layers (~85 nm) as shown in Fig. 4(b), confirming the precise registration of the oriented microdomains on the BCP surface. The ability to prepare multi-layered cross-linked thin films with accurate registration on the nanometre scale demonstrates the power of using functionalized BCPs and may be further utilized as a new route to fabricate 3-dimensional arrays *via* directed self-assembly.

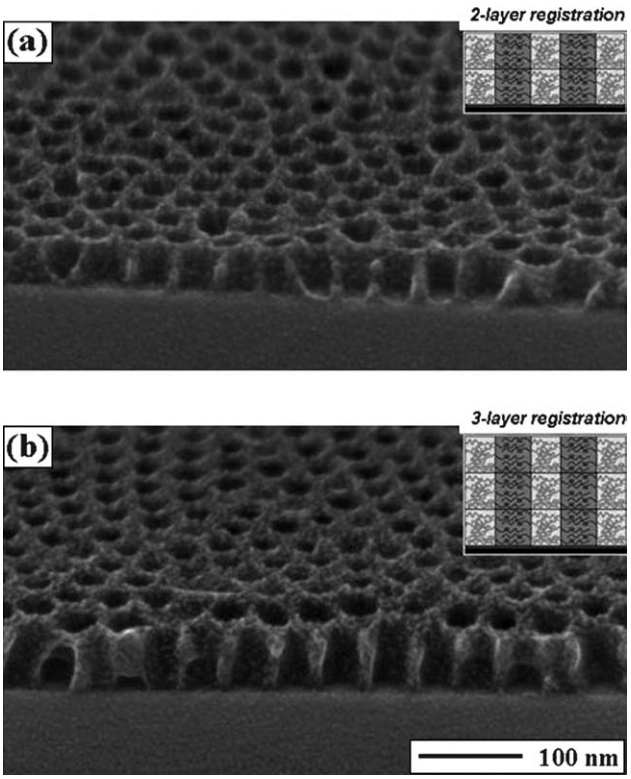

Fig. 4 The schematics for multi-layer fabrication and their SEM images of cross-linked thin films of PS-*b*-PMMA with 3.3 mol% BCB. Cross-sectional images were taken at a tilt angle of 55° for cross-linked thin films fabricated (a) at 2 layers (~54 nm) and (b) at 3 layers (~85 nm), where PMMA microdomains were removed by UV exposure and subsequent rinsing with acetic acid. The microdomain orientation of PS-*b*-PMMA was precisely registered on underlying microdomain arrays oriented normal to the surface.

In summary, polymer thin films from cross-linkable PS-*b*-PMMA copolymers containing the reactive BCB functionality were prepared by thermal annealing and subsequent cross-linking at higher temperatures, leading to robust thermoset, nano-structured thin films. By controlling the extent of cross-linking, either by varying the concentration of BCB or by limiting the extent of cross-linking, a simple route to control the feature size of the microdomains has been shown. Multi-layered cross-linked thin films of the BCP were also fabricated where the microphase separations of adjacent layers were in registry, leading to a propagation of the orientation and ordering of the thin film over large distances. This opens a simple route to generate films with 3-dimensional structure with controlled placement of elements.

Acknowledgements

This work was supported by the Nuclear R&D Programs and APCPI ERC program (R11-2007-050-01004) funded by the Ministry of Science & Technology (MOST), and Ministry of Commerce, Industry and Energy (MOCIE), Korea. Support from the National Science Foundation under the MRSEC program (UCSB MRL, DMR-0520415, UMass MRSEC, DMR-0213695), from a SRC-NRI supplement grant (2006-NE-1549) and the Department of Energy of Basic Energy Science are also gratefully acknowledged.

Notes and references

1 P. Mansky, T. P. Russell, C. J. Hawker, M. Pitsikalis and J. Mays, *Macromolecules*, 1997, **30**, 6810.
2 P. Mansky, C. K. Harrison, P. M. Chaikin, R. A. Register and N. Yao, *Appl. Phys. Lett.*, 1996, **68**, 2586.
3 K. W. Guarini, C. T. Black, Y. Zhang, H. Kim, E. M. Sikorski and I. V. Babich, *J. Vac. Sci. Technol., B*, 2002, **20**, 2788.
4 M. Park, C. Harrison, P. M. Chaikin, R. A. Register and D. H. Adamson, *Science*, 1997, **276**, 1401.
5 E. J. W. Crossland, S. Ludwigs, A. M. Hillmyer and U. Steiner, *Soft Matter*, 2007, **3**, 94.
6 A. Haryono and W. H. Binder, *Small*, 2006, **2**, 600.
7 A. Sperschneider, F. Schacher, M. Gawenda, L. Tsarkova, A. H. E. Müller, M. Ulbricht, G. Krausch and J. Köhler, *Small*, 2007, **3**, 1056.
8 D. H. Kim, K. H. A. Lau, W. Joo, J. Peng, U. Jeong, C. J. Hawker, J. K. Kim, T. P. Russell and W. Knoll, *J. Phys. Chem. B*, 2006, **110**, 15381.
9 J. Lu, D. Chamberlin, D. A. Rider, M. Z. Liu, I. Manners and T. P. Russell, *Nanotechnology*, 2006, **17**, 5792.
10 C. Park, J. Y. Cheng, M. J. Fasolka, A. M. Mayes, C. A. Ross, E. L. Thomas and C. De Rosa, *Appl. Phys. Lett.*, 2001, **79**, 848.
11 A. Knoll, L. Tsarkova and G. Krausch, *Nano Lett.*, 2007, **7**, 843.
12 Y. H. Qiao, D. Wang and J. M. Buriak, *Nano Lett.*, 2007, **7**, 464.

13 I. W. Hamley, *The Physics of Block Copolymers*, Oxford, 1998.
14 E. Huang, L. Rockford, T. P. Russell and C. J. Hawker, *Nature*, 1998, **395**, 757.
15 D. Y. Ryu, K. Shin, E. Drockenmuller, C. J. Hawker and T. P. Russell, *Science*, 2005, **308**, 236.
16 D. Y. Ryu, J. Y. Wang, K. A. Lavery, E. Drockenmuller, S. K. Satija, C. J. Hawker and T. P. Russell, *Macromolecules*, 2007, **40**, 4296.
17 T. Xu, H. C. Kim, J. DeRouchey, C. Seney, C. Levesque, P. Martin, C. M. Stafford and T. P. Russell, *Polymer*, 2001, **42**, 9091.
18 U. Y. Jeong, D. Y. Ryu, J. K. Kim, D. H. Kim, X. D. Wu and T. P. Russell, *Macromolecules*, 2003, **36**, 10126.
19 U. Y. Jeong, D. Y. Ryu, J. K. Kim, D. H. Kim, T. P. Russell and C. J. Hawker, *Adv. Mater.*, 2003, **15**, 1247.
20 E. Drockenmuller, L. Y. T. Li, D. Y. Ryu, E. Harth, T. P. Russell, H. C. Kim and C. J. Hawker, *J. Polym. Sci., Part A: Polym. Chem.*, 2005, **43**, 1028.
21 R. K. O'Reilly, M. J. Joralemon, C. J. Hawker and K. L. Wooley, *J. Polym. Sci., Part A: Polym. Chem.*, 2006, **44**, 5203.
22 Y.-K. Goh, A. K. Whittaker and M. J. Monteiro, *J. Polym. Sci., Part A: Polym. Chem.*, 2007, **45**, 4150.
23 E. Harth, B. Van Horn, V. Y. Lee, D. S. Germack, C. P. Gonzales, R. D. Miller and C. J. Hawker, *J. Am. Chem. Soc.*, 2002, **124**, 8653.
24 S. Blomberg, S. Ostberg, E. Harth, A. W. Bosman, B. Van Horn and C. J. Hawker, *J. Polym. Sci., Part A: Polym. Chem.*, 2002, **40**, 1309.
25 P. Mansky, Y. Liu, E. Huang, T. P. Russell and C. Hawker, *Science*, 1997, **275**, 1458.
26 J. B. He, R. Tangirala, T. Emrick, T. P. Russell, A. Boeker, X. F. Li and J. Wang, *Adv. Mater.*, 2007, **19**, 381.
27 J. Yoon, S. Y. Yang, B. Lee, W. Joo, K. Heo, J. K. Kim and M. Ree, *J. Appl. Crystallogr.*, 2007, **40**, 305.